

caution must be used in interpreting results. Great care must be taken to normalize background characteristics, standardize measurements and interpret results in the context of various gaits utilized by quadrupeds.

## 099

### TIME-COURSE MICRO-CT IMAGING OF BONE CHANGES IN THE RAT ACLTPMx AND MIA MODEL

E. Bartnik<sup>1</sup>, X. Ying<sup>2</sup>, J. Ji<sup>2</sup>, K. Rudolphi<sup>1</sup>, N. Barlow<sup>2</sup>, M.A. Zulliger<sup>3</sup>, K. Arndt<sup>1</sup>

<sup>1</sup>Sanofi-Aventis, Frankfurt, Germany; <sup>2</sup>Sanofi-Aventis, Bridgewater, NJ; <sup>3</sup>Scanco Med., Bruettisellen, Switzerland

**Purpose:** Osteoarthritis (OA) is a disease of the whole joint, including cartilage, synovium, ligaments and bone. The contribution of bone changes to the disease is not well understood. We used  $\mu$ CT imaging to determine the time course of bone parameter changes in the rat Anterior Cruciate Ligament Transection plus Partial Medial Meniscectomy (ACLTPMx) model and the rat Monoiodoacetate (MIA) model.

**Methods:** The ACLTPMx operation was used to induce OA-like changes. 70 male Lewis rats were assigned to the following groups: 3, 7, 14, 28, 42 days post ACLTPMx surgery, no surgery and sham surgery. At 3, 7, 14, 28, 42 days post ACLTPMx animals were sacrificed.

In a second set of animals [n=3], 1 mg/joint of MIA was injected into the knee to induce joint damage. 17 and 39 days after injection, NaCl-control and MIA-injected animals were sacrificed. For the bone/cartilage  $\mu$ CT imaging, each distal femur was immersed in an ionic CT contrast agent solution (30% Hexabrix in phosphate buffered saline) for 25 min at  $\sim 21^\circ\text{C}$ , then the surface liquid absorbed and the femur was immediately transferred to the  $\mu$ CT system (SkyScan 1172, SkyScan, Belgium), with the setting of 50kVp/200 $\mu$ A, 0.5 mm aluminium filter and 20  $\mu\text{m}^3$  imaging voxel size. The images were imported and analyzed using SCANCO Medical Evaluation Software (SCANCO Medical AG, Switzerland). Reference average epiphyses, generated after registration and summation of all studied epiphyses, served as guides to determine regions of interest (weight bearing, central areas of the medial and lateral tibial plateau, Fig. 1) for the medial and lateral tibial plateaus, which were overlaid onto each individual epiphysis. Using the defined ROIs, the analyzed structures were cut cookie-cutter-style and further analyzed to provide standard morphometric bone parameters.



Figure 1. Regions of interest overlaid on the medial (M) and lateral (L) tibial plateau.

**Results:** Bone volume, BV/TV, structural model index (SMI) and marrow thickness (trabecular separation Tb.Sp) tend to increase with the age of the animals. ACLTPMx induced changes within the epiphysis were recognizable 7 days after the ACLTPMx procedure, reaching a maximum around 14 days and subsequently subsiding. By 42 days after the operation, the ACLTPMx induced changes had returned to normal. Tb:Sp reflected the most prominent ACLTPMx induced effect, but did not reach statistical significance comparing values at Day 3 with values at Day 14.

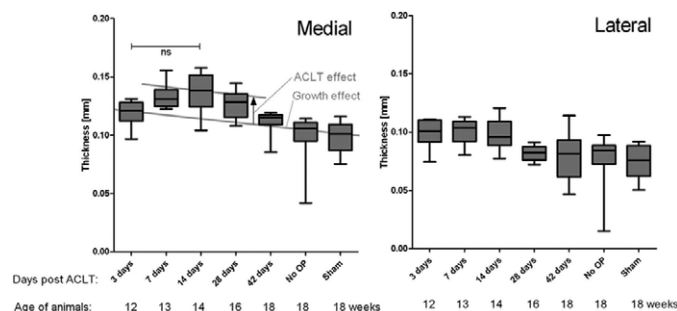


Figure 2. Time course of bone marrow thickness within the ROI in the medial and lateral epiphyses at different times after ACLTPMx.

MIA induced far greater effects on bone parameters compared to ACLTPMx.

17 days after MIA injection, bone volume and mean thickness of bone structures had increased (comparing NaCl and MIA injected groups), whereas trabecular connectivity had decreased. At 39 days the differences were much less prominent.

**Conclusions:**  $\mu$ CT extends our ability to monitor changes in OA models to bone parameters. Trends of bone parameter changes are evident for both the ACLTPMx as well as for the MIA model. The most obvious changes correlate with the age of the animals and thus should reflect growth-related changes. These were seen in both the medial and the lateral tibial compartment. The changes seen as a result of the ACLTPMx occurred only in the medial compartment, where most of the cartilage damages occur in this model. These changes appear 7 days after surgery hinting at the adaptability of bone structures. Although the changes were quite evident, their range of fold-change is rather small not reaching statistical significance. Therefore one needs to refine those measurements, i.e. by further defining the ROIs to use those parameters to describe the effect of structure modifying compounds.

## 100

### CAN ANIMAL MODELS APPROXIMATE THE CHARACTERISTICS OF HUMAN SUBCHONDRAL BONE?

M. Hurtig, M. Lowerison, S. Allendorf, A. Bell  
Univ. of Guelph, Guelph, ON, Canada

**Purpose:** To characterize the subchondral bone plate (SBPlate) in normal animals and humans. Our hypothesis was that the human subchondral bone plate is unique and not comparable to quadruped animals. The SBPlate is important in the understanding of osteoarthritis (OA) initiation and progression as both sclerosis and porosity have been implicated as contributing factors. The SBP is also important because it constitutes a barrier to extrinsic cartilage repair. Animal models of cartilage repair and regeneration are used to validate new cell- and biomaterial-based interventions.

**Methods:** Normal medial femoral condyles from adult humans and animals (n=4 each species) underwent microCT imaging at 45 $\mu$  resolution (GE Locus Explore). The resulting images were analyzed using 3 $\times$ 3 $\times$ 10 mm regions of interest (ROIs) created starting at the tidemark and extending through the SBPlate where bone mineral density (BMD), tissue mineral density (TMD) and bone volume fraction (BVf) were determined using Microview 2.2 (ABA). Additional depth-wise analyses of these regions were done by expressing the mean voxel densities in each horizontal slice by depth starting at the tidemark. Dicom images were converted to text files and truncated to the POIs, then processed through custom scripts in Python 3.1.1 and R ([www.r-project.org](http://www.r-project.org)). These scripts execute calibrations to convert voxel HU to BMD in mg/cc or apply a user controlled threshold to generate BVf (%). Data from depth-wise analyses was plotted by distance from the articular surface. In addition, rate of change of BMD, TMD, and BVf was investigated as a way of determining the subchondral plate thickness.

**Results:** Human SBP BMD and TMD in standard ROIs was significantly lower (p<0.05) than all animal species except the sheep and dog. Human BVf was the lowest of all species (Figs. 1 and 2). Rate of change in BMD

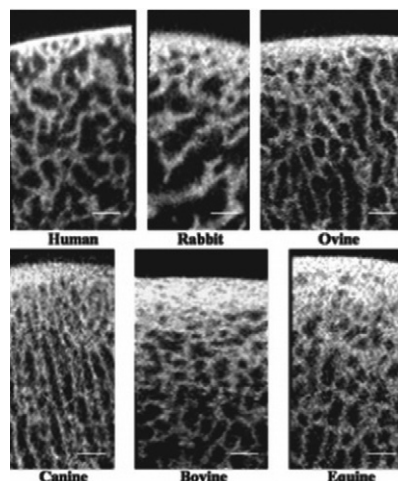


Figure 1

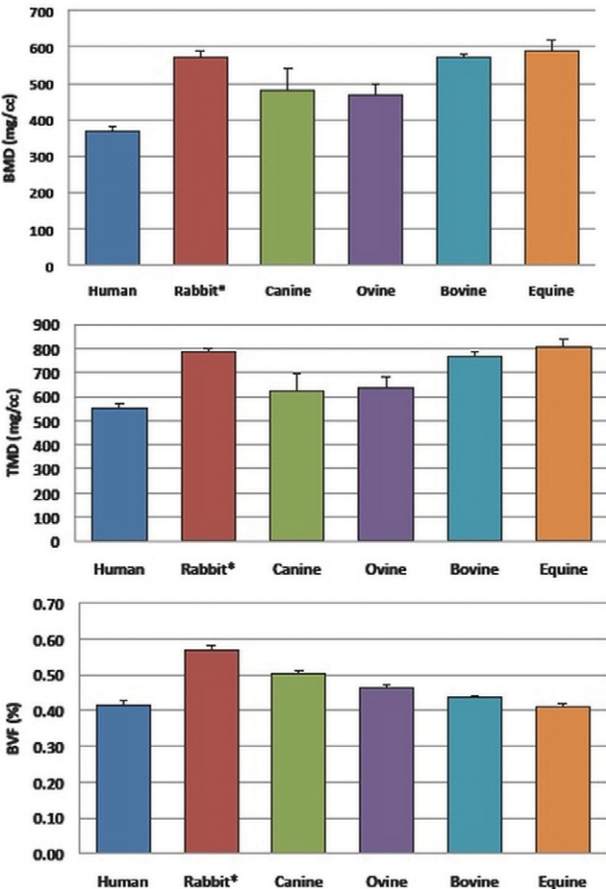


Figure 2

by depth showed that no species was similar to the human with respect to SBP thickness (Table 1) or mineralization gradient (Fig. 3) though the dog was closest. In early human osteoarthritis the thickness and mineral density of the SBP was significantly ( $p<0.01$ ) expanded.

Table 1

SPECIES	Subchondral Plate Thickness Estimate by BMD Rate of Change	
	Average (mm)	Std. Deviation
Human-normal	0.49	± 0.02
Human-OA	1.25	+ 0.30
Rabbit	0.72	± 0.03
Canine	0.66	± 0.04
Ovine	0.77	± 0.01
Equine	1.23	± 0.04
Bovine	1.30	± 0.03

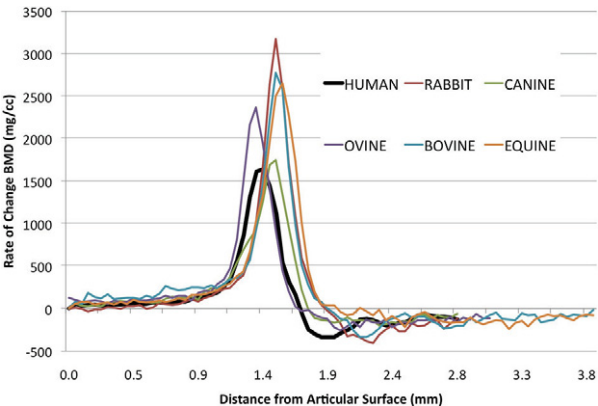


Figure 3

**Conclusions:** In normal human femoral condyles, the SBP is comprised of the condensation of approximately two horizontal trabeculae after which there are many communicating marrow spaces. This represents little or no barrier to the ingress of marrow constituents after a breach in the subchondral bone. In osteoarthritis the sclerotic SBP presents a substantial barrier to marrow stimulation procedures (data not shown). By contrast, all animals have subchondral bone plates that are thicker, more mineralized and have more bone volume compared to similar human tissue. Thus, these are not valid models of the normal human SBP, but instead could be considered an approximation of sclerotic human subchondral bone. These data explain why the response to injury or microfracture in large species such as the horse may underestimate human reparative capacity.

101

**CALCITONIN PREVENTS THE LOSS OF CONNECTIVITY AND COMPLEXITY OF TRABECULAR SUBCHONDRA BONE IN EARLY STAGES OF CANINE OSTEOARTHRITIS**

C. Behets<sup>1,2</sup>, D. Chappard<sup>3,4</sup>, J.-P. Devogelaer<sup>1,5</sup>, D.H. Manicourt<sup>1,5</sup>  
<sup>1</sup>Université Catholique de Louvain, Brussels, Belgium; <sup>2</sup>Dept. of Anatomy, UCL, Brussels, Belgium; <sup>3</sup>Faculté de médecine, Angers, France; <sup>4</sup>INSERM U922-LHEA, Angers, France; <sup>5</sup>Dept. of Rheumatology, Brussels, Belgium

**Purpose:** to assess changes in the three-dimensional micro-architecture of subchondral trabecular (Tb) bone in canine experimental osteoarthritis (OA) and to evaluate to what extent calcitonin (CT) might affect micro-architectural changes of OA subchondral bone.

**Methods:** after transection of the anterior cruciate ligament (ACL) of their right knee, mongrel dogs received either daily calcitonin (CT; n=7) or daily placebo (PL; n=7). At day 84 after surgery, animals were killed and cartilage changes were graded in both operated (OP) and non-operated (N-OP) control knees. High-resolution micro-computed tomography by synchrotron radiation, the gold standard for bone micro-architecture imaging, was used to assess changes in different regions of interest of the subchondral Tb bone of tibial plateaus (TPs). Besides bone volume fraction (BV/TV) and Tb thickness (TbTh), we measured Tb bone spacing (TbSp) that measures the mean size of marrow cavities, as well as Tb bone pattern factor (TbP) and interconnectivity index (ICI) which both reflect the amount of closed/open marrow cavities. Statistics included a 2x2 factorial analysis with +/-CT as one factor and +/-ACL as the other.

**Results:** N-OP knees were normal in both groups. In the PL-treated group, ACL knees all exhibited OA changes which predominated in the medial knee compartment. Further, compared to N-OP knees, significant changes in parameters of bone micro-architecture were significantly changed in medial TP, but not in lateral TP of OP knees: thus, while BV/TV and TbTh both were significantly decreased ( $p<0.05$ ), TbSp, ICI and TbP were markedly increased ( $p<0.01$ ). In contrast, in the CT-treated group, cartilage OA lesions of OP knees were significantly reduced ( $p<0.01$ ), and there was no statistically significant difference in BV/TV, TbTh, TbSp, ICI and TbP between OP and N-OP knees. On the other hand, the thickness of subchondral cortical bone plate was unaffected by surgery and treatment.

**Conclusions:** the loss of trabeculae in the subchondral bone of OA knees was associated with a loss of complexity and connectivity of the Tb network. Since they were only observed in medial TPs where cartilage OA lesions predominated, these micro-architectural bony changes which are known to increase bone fragility and to decrease bone strength are likely to contribute to the breakdown of the overlying cartilage, a contention further strengthened by the observation that CT, a potent inhibitor of osteoclastic bone resorption, reduced OA lesions and concomitantly prevented the bone loss by preserving Tb bone volume and Tb network connectivity. These observations add further support to the potential therapeutic use of CT in human

102

**CHARACTERIZATION OF A NOVEL OSTEOARTHRITIS ANIMAL MODEL AND EARLY PREVENTION OF INFLAMMATION POST-SURGERY**

K.D. Huebner, N.G. Shrive, C.B. Frank  
Univ. of Calgary, Calgary, AB, Canada

**Purpose:** The knee is a unique organ, which is highly susceptible to injuries because of the loads and stresses placed on it. While ligament instability appears to cause repeated joint injuries and can lead to Osteoarthri-